Spin polarization of the low-density three-dimensional electron gas

F. H. Zong, C. Lin, and D. M. Ceperley
Department of Physics and NCSA, University of Illinois at Urbana-Champaign, Urbana, Illinois 61801
(Received 17 May 2002; published 20 September 2002)

To determine the state of spin polarization of the three-dimensional electron gas at very low densities and zero temperature, we calculate the energy versus spin polarization using diffusion quantum Monte Carlo methods with backflow wave functions and twist averaged boundary conditions. We find a second-order phase transition to a partially polarized phase at $r_s \sim 50 \pm 2$. The magnetic transition temperature is estimated using an effective mean-field method, the Stoner model.

DOI: 10.1103/PhysRevE.66.036703 PACS number(s): 02.70.−c, 71.10.Ca, 71.10.Hf, 05.30.Fk

I. INTRODUCTION

The three-dimensional homogeneous electron gas, also known as the fermion one component plasma or jellium, is one of the simplest realistic models in which electron correlation plays an important role. Despite years of active research, the properties of thermodynamic phases of the electron gas are still not known at intermediate densities [1]. In this paper, we study the spin polarization phase transition of the three-dimensional electron gas at zero temperature with recently improved quantum Monte Carlo (QMC) methods.

There has been recent interest in the low-density phases spurred by the observation of a ferromagnetic state in calcium hexaboride (CaB_6) doped with lanthium [2]. The magnetic moment corresponds to roughly 10% of the doping density. The temperatures (600 K) and densities ($7 \times 10^{19}/\mathrm{cm}^3$) of this transition are in rough agreement with the predicted transition in the homogeneous electron gas [1]. However, to make a detailed comparison, it is necessary to correct for band effects. For example, conduction electrons are located at the *X* point of the cubic band structure and thus have a sixfold degeneracy. The effective mass of electrons at this point and the dielectric constant are also changed significantly from their vacuum values [3]. These effects cast doubt on the viability of the electron gas model to explain the observed phenomena. Excitonic models have been proposed to explain the ferromagnetism [4]. Whatever the interpretation of ferromagnetism in CaB_6, the determination of the polarization energy of the electron gas is an important problem because of the importance of the model.

The ground-state properties of the electron gas are entirely determined by the density parameter $r_s = a/a_0$ where $4\pi\rho a^3/3 = 1$ and a_0 is the bohr radius, possibly changed from its vacuum value by band effects. In effective Rydbergs, the Hamiltonian is

$$H = -\frac{1}{r_s^2}\sum_{i=1}^{N} \nabla_i^2 + \frac{2}{r_s}\sum_{i<j}\frac{1}{|\mathbf{r}_i - \mathbf{r}_j|} + \text{const.} \qquad (1)$$

Note that the kinetic energy scales as $1/r_s^2$ and the potential energy scales as $1/r_s$ so that for small r_s (high electronic density), the kinetic energy dominates, and the electrons behave like an ideal gas; in the limit of large r_s, the potential energy dominates and the electrons crystallize into a Wigner crystal [5]. There is a first order freezing transition [6] at $r_s \approx 100$.

Considering now the spin degrees of freedom, at small r_s, electrons fill the Fermi sea with equal number of up spin and down spin electrons to minimize the total kinetic energy and thus the total energy; the system is in the paramagnetic state. As the density decreases and before the freezing transition, there is a possibility that the electrons become partially or totally polarized (ferromagnetic). The spin polarization is defined as $\zeta = |N_\uparrow - N_\downarrow|/N$, where $N_\uparrow$ and $N_\downarrow$ are the number of up and down spin electrons, respectively, and $N = N_\uparrow + N_\downarrow$. For paramagnetic phase $\zeta = 0$ and for ferromagnetic phase $\zeta = 1$.

This polarization transition was suggested by Bloch [7] who studied the polarized electronic state within the Hartree-Fock (HF) approximation. He found the ferromagnetic state favored over paramagnetic state for $r_s > 5.45$, almost within the density of electrons in metals. However, HF is not accurate for $r_s > 0$.

More accurate energies became available with the development of Monte Carlo methods for many-fermion systems. Ceperley [8] using variational Monte Carlo with a Slater-Jastrow trial function determined that the transition between the polarized and unpolarized phase occured at $r_s = 26 \pm 5$. Using a more accurate method, diffusion Monte Carlo (DMC) [6], it was estimated that the polarized fluid phase is stable at $r_s = 75 \pm 5$. An extension to this work [9] found the $\zeta = 0.5$ partially polarized fluid becomes stable at roughly $r_s \approx 20$ and the completely polarized state is never stable.

Recently Ortiz *et al.* [1] applied similar methods [10] to much larger systems ($N \leqslant 1930$) in order to reduce the finite-size error. They concluded that the transition from the paramagnetic to ferromagnetic transition is a continuous transition, occurring over the density range of $20 \pm 5 \leqslant r_s \leqslant 40 \pm 5$, with a fully polarized state at $r_s \geqslant 40$.

Due to the very small energy differences between states with different polarizations, systematic errors greatly affect the QMC results. Recent progress in the quantum simulation methods makes it possible to reduce these errors. Kwon *et al.* [11] found that a wave function incorporating backflow and three-body (BF-3B) terms provides a more accurate description: they obtained a significantly lower variational and fixed-node energy. In another advance of technique, twist-

averaged boundary conditions (TA) [12] have been shown to reduce the finite-size error by more than an order of magnitude, allowing one to obtain results close to the thermodynamic limit using results for small values of N. In this paper, we apply these improved methods to the polarization transition in the three-dimensional electron gas. We first describe the simulation method, and then, the results.

II. METHODS

The most accurate QMC method [13] at zero temperature is projector or DMC: one starts with a trial function and uses $\exp(-tH)$ to project out the ground state using a branching random walk. Fermi statistics pose a significant problem for the projection method, since exact fermion methods such as transient estimate or release-node QMC suffer an exponential loss of efficiency for large numbers of particles. For this reason, the fixed-node approximation is normally used, obtaining the best upper bound to the energy consistent with an assumed sign of the wave function. The generalization of the fixed-node method to treat complex-valued trial functions is known as the fixed-phase approximation [14].

In the simpler, but less accurate variational Monte Carlo method (VMC), one assumes an analytic form for a trial function $\Psi_T(R)$ and samples $|\Psi_T(R)|^2$ using a random walk. An upper bound to the exact ground-state energy is the average of the local energy $E_L(R)=\Psi_T(R)^{-1}\mathcal{H}\Psi_T(R)$ over the random walk.

The trial wave function plays a very important role in these two methods. With a better trial wave function, not only is the variational energy lower and closer to the exact energy, but also the variance of the local energy is smaller so that it takes less computer time to reach the desired accuracy level. The trial wave function is also important in fixed phase DMC because the solution is assumed to have the same phase as the trial function. One then solves for the modulus. This implies that the DMC energy lies above the exact ground-state energy by an amount proportional to the mean squared difference of the phase of the trial function from the exact phase. As this is the only uncontrolled approximation, it is important to carefully optimize the assumed trial wave function.

For a homogeneous system, the noninteracting (NI) wave function consists of a Slater determinant of single-electron plane waves orbitals. To incorporate electron correlation, one multiplies the NI wave function by a pair wave function, obtaining the so-called Slater-Jastrow (SJ) form. To construct a better trial function, one incorporates backflow and three-body effects [11]. The particle coordinates appearing in the determinant become quasiparticle coordinates,

$$\mathbf{x_i}=\mathbf{r_i}+\sum_{j\neq i}^{\mathbf{N}}\eta(\mathbf{r_{ij}})(\mathbf{r_i}-\mathbf{r_j}). \tag{2}$$

The Slater determinant is then $D=\det(e^{i\mathbf{k_m}\cdot\mathbf{x_n}})$ where $\eta(r_{ij})$ is a function to be optimized. Then the (BF-3B) wave function is

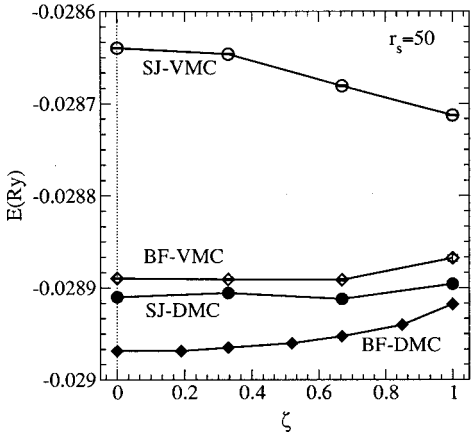

FIG. 1. Energy vs spin polarization at $r_s=50$ for 54 electrons using TA with 10^3 twist values. Compared are calculations with SJ and BF-3B wave functions and with two QMC methods: VMC and DMC.

$$\Psi_T(R)=D_\uparrow D_\downarrow\exp\left(-\sum_{i<j}^{N}\tilde{u}(r_{ij})-\frac{\lambda_T}{2}\sum_{i=1}^{N}\mathbf{G_i^2}\right), \tag{3}$$

where

$$\mathbf{G_i}=\sum_{j\neq i}^{\mathbf{N}}\xi(\mathbf{r_{ji}})(\mathbf{r_j}-\mathbf{r_i}) \tag{4}$$

and

$$\tilde{u}(r)=u^{RPA}(r)-\lambda_T\xi^2(r)r^2+\gamma(r). \tag{5}$$

Here $D_\uparrow$ and $D_\downarrow$ are the determinants for the up spin and the down spin electrons, $\xi(r)$ is the three-body correlation function, and $\tilde{u}$ is the Jastrow correlation function. For the electron gas an accurate analytic form [15], $u^{RPA}(r)$, has as low an energy [8] as those with optimized parameters. In the presence of three-body correlation, the random-phase approximation (RPA) two-body term is supplemented with an extra Gaussian function $\gamma(r)$. Please refer to Kwon *et al.* [11] for further details concerning this wave function. We used optimized Ewald sums [16] both for the potential and for the correlation factor so as to have the correct long wave length behavior.

Though the computational cost for BF-3B wave function is somewhat greater than the simple SJ wave function and there is the added cost of optimization for BF-3B wave function, we found accurate trial wave functions crucial to compute the small energy differences between different polarization states. We optimized the parameters by minimizing a combination of the energy and the variance for each density and polarization. Figure 1 shows the energy vs polarization at $r_s=50$ using different trial functions and simulation methods. The SJ trial function with VMC has the highest energy for all polarizations and at this level of accuracy finds the fully polarized phase to be stable, in agreement with earlier VMC calculations [8]. However, using the best BF-3B trial function, the variational energies are lowered significantly with the unpolarized energy dropping more than the polar-

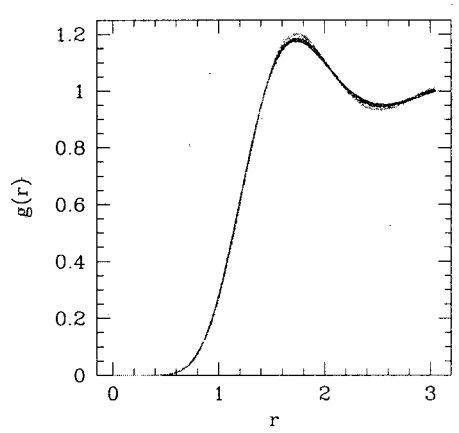

FIG. 2. The pair correlation function for several polarizations at $r_s=50$ using DMC. The various curves are for $\zeta=0,0.33,\ 0.67,\ 1$ with the structure increasing with spin polarization.

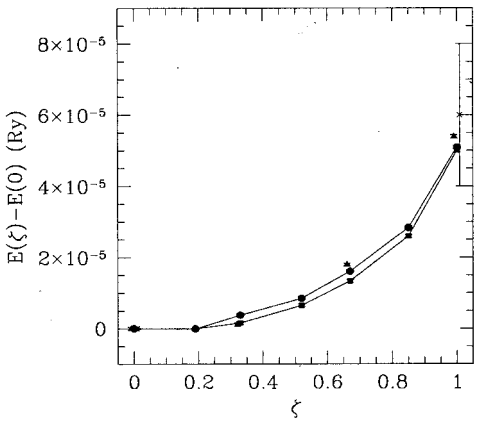

FIG. 3. The polarization energy for various sized systems at $r_s=50$ using TA and DMC (circle, 54; square, 108; and triangle, 162). The point at $\zeta=1$ with the large error bar is from Ceperley and Alder [6]. Other errors are less than 10^{-6}.

ized case so that the polarized phase is no longer stable. DMC calculations confirm this result. Note that the DMC energies determined using the NI phases (or nodes) give energies lower than the BF-3B variational energies, confirming the importance of accurate DMC calculations. The use of BF-3B wave functions with DMC leads to the lowest ground-state energies, hopefully, very close to the exact energy.

After the effect of the nodes, the dependence of the energy on the number of electrons is the largest systematic error. Within periodic boundary conditions (PBC), the phase picked up by the wave function as a particle makes a circuit across the unit cell, is arbitrary. General boundary conditions are

$$\Psi(\mathbf{r}_1+L,\mathbf{r}_2,\ldots)=e^{i\theta}\Psi(\mathbf{r}_1,\mathbf{r}_2,\ldots), \tag{6}$$

where L is a lattice vector of the supercell. If the twist angle θ is averaged over, most single-particle finite-size effects arising from shell effects in filling the plane wave orbitals, are eliminated. This is particularly advantageous for polarization calculations since shell effects dominate the polarization energy. The extra effort in integrating over the twist angles is minimal, since the various calculations all serve to reduce the final variance of the computed properties. The effect of boundary conditions is examined in detail in the paper of Lin *et al.* [12]

There is a further size effect in the calculation of the potential energy due to a charge interacting with its correlation hole in neighboring supercells as shown in Fig. 6 of Lin *et al.* [12]. To correct this, we fit the energies versus N using the expansion

$$E_N=E_\infty+\frac{a_1}{N}+\frac{a_2}{N^2}+\cdots. \tag{7}$$

For unpolarized systems, the fitted E_∞ agrees with the previous non-twist-averaged (PBC) result determined using extrapolations based on Fermi liquid theory (FLT). As shown in Fig. 2, the correlation hole is only weakly dependent on spin polarization at low density: the peak of $g(r)$ only changes from 1.175 to 1.190 as the system goes from unpolarized to polarized. Hence, the potential size effect hardly changes the spin polarization energy. Figure 3 shows the polarization energies for $N=54,\ 108,\ 162$. With TA boundary conditions, there is a remarkable insensitivity to the number of electrons. Even though the system size is increased threefold, the change in the energy versus polarization is almost undetectable. Considering only the leading $1/N$ correction, we estimated E_∞ with $N=54$ and $N=108$.

Also shown in Fig. 3 is the estimate of the polarization energy from Ceperley and Alder [6]. In that work, size effects were estimated with Fermi liquid corrections. Rather than BF-3B wave functions, corrections using the potentially exact, release-node method were used. The results with PBC and fixed-node (FN) -DMC are in agreement with the present fixed-phase (FP) -DMC calculations. However, the present results have an error bar more than an order of magnitude smaller than those of Ceperleya and Alder, primarily due to increased computer performance.

Though PBC with FLT corrections are adequate for unpolarized and fully polarized systems, the precision is limited for intermediate polarizations. To estimate finite size effects within FLT, one must perform accurate DMC simulations for widely varying system sizes. In the paper of Ortiz *et al.* [1], the simulation size varied from $725\leqslant N\leqslant 1450$. Within DMC it is very time consuming to ensure uniform accuracy independent of particle number, so that one typically determines size effects within VMC, using the more approximate SJ trial functions. As we have seen in Fig. 1, the SJ trial functions are unreliable at low densities. TA boundary conditions allow a much better way to estimate energies in the thermodynamic limit of partially polarized Fermi liquids since the number of electrons can be held fixed as the spin polarization varies. Small system sizes, allowing the use of more accurate but expensive trial functions and even exact fermion methods, give precise estimates of the spin polarization energy in the thermodynamic limit.

In Fig. 4 we compare the total energy for $r_s=40$ calculated with DMC and TA and extrapolated to the thermodynamic limit with the calculation of much larger systems (N

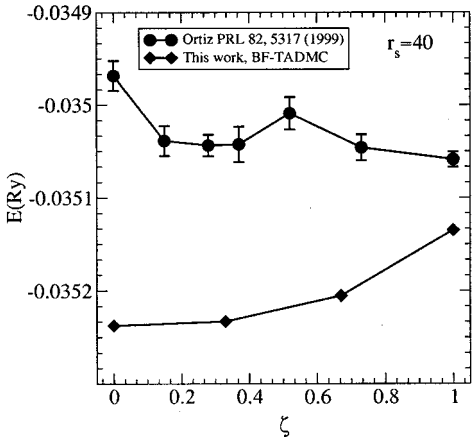

FIG. 4. Comparison of this work with that of Ortiz *et al.* [1]. The filled diamonds are DMC simulations with TA and BF-3B wave functions (this work). The filled circles are DMC with PBC and SJ wave function [1]. All energies are extrapolated to the thermodynamic limit. Errors are given in Table I and are smaller than the size of the points.

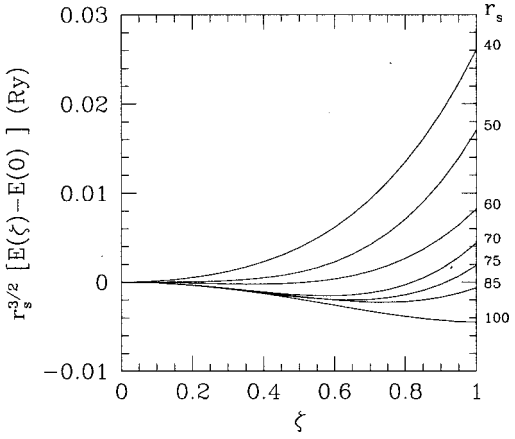

FIG. 5. The spin polarization energy of the 3DEG times $r_s^{3/2}$ in Ry/electron at various densities using a polynomial fit to the data in Table I. The density, r_s, is denoted on the right axis.

$=725$) of Ortiz *et al.* [1] The BF-3B energies are lower energy and show a different polarization energy: Ortiz's calculation finds that the polarized or partially polarized phase is stable at this density, while we find the unpolarized phase is stable. This difference is due to the backflow correlations in the trial wave function. Although backflow energies are small, they favor the unpolarized state and hence are crucial for accurate determination of the polarization transition.

III. RESULTS

We carried out computations of the spin polarization energies at electronic densities $40 \leqslant r_s \leqslant 100$. At each density, we performed DMC calculations with $N=54$ and $N=108$ electrons using 10^3 twist angles. The time step was adjusted so that the DMC acceptance ratio was in the range 98–99 %. Note that when calculating the polarization energy, most time step errors will cancel out of the polarization energy. Thus systematic errors in the polarization energy are much smaller than in the total energy. We then extrapolated the energy to the thermodynamic limit using Eq. (7). The energies are given in Table I.

We then fit the energy versus polarization to a quadratic polynomial in ζ^2. The results are shown in Fig. 5. A polarization transition is evident. At $r_s=40$, the system is still paramagnetic, with the unpolarized phase stable. As the density decreases, at $r_s \approx 50$, the system becomes unstable with respect to spin fluctuations. The partially polarized states become stable at $r_s \geqslant 60$. As the electronic density continues to decrease, the fully polarized state has a lower energy with respect to unpolarized state at $r_s \geqslant 80$, however, we find that the partially polarized state has an even lower energy.

In Fig. 6 is shown the predicted square of the optimal polarization versus density. We find that the equilibrium polarization is described by $\zeta^2=(r_s-r_s^*)/62$ with the critical density $r_s^*=50\pm 2$. As the density decreases, the stable state becomes more and more polarized, becoming fully polarized at the freezing density, $r_s \approx 100$. Quantum critical fluctuations, not present in systems with $N \leqslant 162$, could modify the behavior of the spin polarization energy near the critical density.

The quoted error bar on the critical density estimates the statistical errors, not the systematic errors arising from the fixed-phase approximation. The experimental and theoretical results on polarized helium warn against placing too much confidence in the estimate of the polarization transition. Even using the accurate optimized BF-3B wave functions, the magnetic susceptibility in liquid ^{3}He does not agree with

TABLE I. Energy of the 3DEG computed using TA-DMC and extrapolated from $N=54$ and $N=108$ with 10^3 twist angles. Energies are in Ry/electron. The numbers in parentheses are standard errors in units of 10^{-8} Ry.

$r_s \backslash \zeta$	0.0	0.185	0.333	0.519	0.667	0.852	1.0
40	−0.03523748(60)		−0.03523295(67)		−0.03520539(67)		−0.03513483(72)
50	−0.02889900(62)	−0.02889900(66)	−0.02889962(68)	−0.02889449(70)	−0.02888835(62)	−0.02887542(70)	−0.02884983(81)
60	−0.02452017(44)	−0.02451866(51)	−0.02452031(48)	−0.02451963(50)	−0.02451747(42)	−0.02451188(46)	−0.02450167(46)
70	−0.02131429(41)	−0.02131381(40)	−0.02131621(39)	−0.02131716(37)	−0.02131593(37)	−0.02131332(39)	−0.02130667(37)
75	−0.02001137(35)	−0.02001191(37)	−0.02001376(36)		−0.02001434(44)		−0.02000878(33)
85	−0.01784017(30)		−0.01784152(32)		−0.01784300(32)		−0.01784109(32)
100	−0.01535357(30)		−0.01535340(30)		−0.01535639(26)		−0.01535761(26)

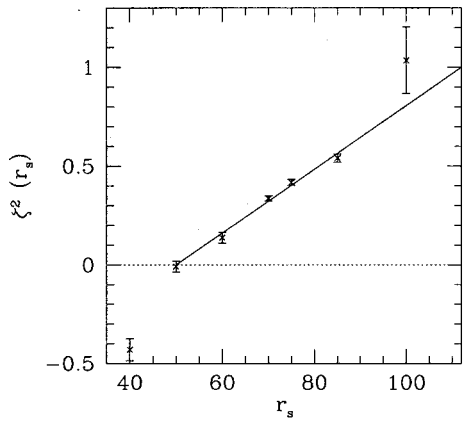

FIG. 6. The square of the spin polarization vs r_s. The curves were obtained using fits in Fig. 4. The line is a fit though the points. The value at $r_s=40$ was obtained by extrapolation from physical values of ζ.

experiment at low pressure and the polarized phase is nearly degenerate with the unpolarized phase at the freezing density [17]. The present results also do not preclude the existence of phases with other order parameters such as superfluids, as occurs in the ground state of liquid ^{3}He. In fact, it is rather likely that the ground state of the electron gas will have such a phase at the lowest fluid densities.

However, examination of the variance of the trial function suggests that the result for the electron gas may be more reliable than for liquid ^{3}He. Shown in Fig. 7 is the variance of the trial function at $r_s=50$ for both the SF and the BF-3B functions. Although the variance of the SJ trial function depends on spin polarization, that of the BF-3B does not. Such is not the case [17] with liquid ^{3}He. Arguments based on variance extrapolation [18] suggest that the DMC calculations with BF-3B phases should be more reliable than in liquid ^{3}He.

IV. THE PHASE DIAGRAM

One can use the calculated energies to estimate the finite temperature behavior within the Stoner model [19], arising in

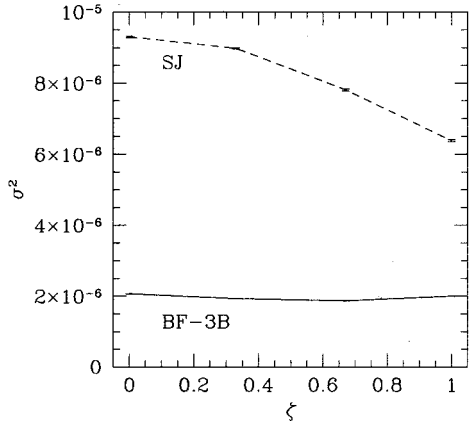

FIG. 7. The variance of the SJ and BF-3B trial function as a function of spin polarization at $r_s=50$ using TA and VMC with $N=54$.

the theory of itinerant magnetism [20]. The Stoner model differs from the Hartree-Fock approximation by replacing the Coulomb interaction by a zero range one, a repulsive delta function potential: $\Sigma_{i<j} g\,\delta(r_{ij})$. One can view this approach as the first step to a full Fermi-liquid description of the quasiparticle interactions, and use the QMC data to determine the strength of those interactions. One expects that the Slater-Jastrow trial function has screened off the long-range interaction, leaving only a short-ranged spin-dependent term that can be modeled by a contact interaction.

In the Stoner model, the energy is evaluated within the mean-field (Hartree-Fock) approximation using the NI wave function. The energy at zero temperature in the thermodynamic limit is

$$E \propto (1+\zeta)^{5/3} + (1-\zeta)^{5/3} + 0.054 g r_s^2 (1-\zeta^2). \tag{8}$$

For $gr_s^2 < 20.5$ the system has an unpolarized ground state and for $gr_s^2 > 24.4$ the ground state is ferromagnetic. For intermediate couplings, the ground state has a partial spin polarization at zero temperature, similar to the observed behavior of the electron gas at low density.

Although the polarizations are qualitatively correct, the above functional form does not fit well the DMC data (i.e., from Table I). In addition, assuming that g does not have a very strong density dependence, the Stoner model predicts that the partially polarized density range should be quite narrow, from $50 \leqslant r_s \leqslant 54$, while as the QMC results indicate a much broader density range. Certainly, the assumption of a zero-range interaction of quasiparticles is too restrictive. However, we note that in the case of the three-dimensional Ising model, the mean-field estimate of the critical temperature is approximately 20% greater than the exact value, suggesting that the Stoner model will give a reasonable estimate of the transition temperature if the effective couplings are determined from the QMC ground-state energies.

We use the Stoner model to make an estimate of the transition temperature of the polarized phase as follows. The free energy [21] in a fixed volume V in the Stoner model is

$$F = F_0(N_\downarrow) + F_0(N_\uparrow) + \frac{g N_\uparrow N_\downarrow}{V}, \tag{9}$$

where the free particle free energy for a single spin species at large N is

$$F_0(N) = N\mu - k_B T \sum_k \ln(1 + e^{-\beta(e_k-\mu)}). \tag{10}$$

The chemical potential μ of each spin species is determined by the number of particles with that spin. At each density, we perform a three parameter linear least squares fit of the energies in Table I, to determine the zero of energy, the effective mass, and the spin coupling parameter g using Eq. (8). Then, we numerically calculate the temperature at which the system becomes polarized by determining when the spin

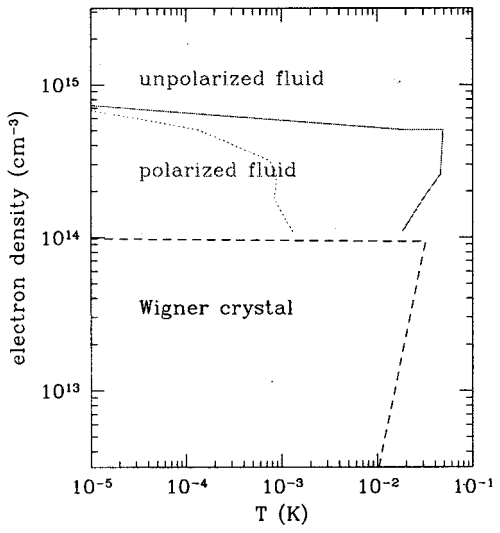

FIG. 8. The phase diagram of the electron gas. Conversion to units of cm and K was done using $a_0 = 1.3$ nm and Ry$=250$ K using estimates [3] of the effective mass and the dielectric constant of SrB_6. The solid line is the mean-field estimate of the magnetic transition temperature from the Stoner model, where the spin interaction is estimated from the zero temperature QMC data. The dotted line is the energy difference between the unpolarized and partially polarized system.

stiffness of the unpolarized system vanishes, i.e., $d^2F/d\zeta^2 = 0$.

Figure 8 is the estimated phase diagram of the electron gas. In this diagram, the effective mass and dielectric constant for SrB_6, a closely related material to CaB_6, have been used [3] to convert to units of K and cm^3. Note that both the temperatures and densities of our calculated magnetic transition are four orders of magnitude smaller than that found experimentally [2] in CaB_6. Even assuming errors because of uncertainties in material properties and from the mean-field estimate of T_c, these estimates are very difficult to reconcile with experiment, apparently ruling out an electron gas model of ferromagnetism in this material. Also plotted on the phase diagram is the energy difference between the partially polarized fluid and the unpolarized fluid as another estimate of the magnetic transition temperature. Finite temperature QMC calculations would be desirable to confirm the mean-field estimate of T_c. A rough estimate of the limit of stability of the Wigner crystal [22] is also shown.

Tanaka and Ichimaru [23] have computed the polarization phase diagram of the electron gas both at zero and nonzero temperature using an integral equation method. At zero temperature they obtain a result similar to that of Ortiz *et al.* [1], with a continuous transition at $r_s \approx 20$ and a fully polarized fluid state at a slightly higher density $r_s \approx 22$. Apparently this approach, built on local field corrections to free fermion response functions, is biased by the initial Hartree-Fock assumption and overemphasizes the tendency for ferromagnetism.

There is recent work on the low-density electron gas in two-dimensions (2D), studying both the Fermi liquid [24] and the Wigner crystal phase. Using QMC techniques in the liquid phase, a polarized phase is found to be stable between $26 \leqslant r_s \leqslant 35$, though the energy differences are even smaller than in 3D. The partially polarized phase is never stable. In the two-dimensional Wigner crystal, path integral methods [25] were used to derive directly the spin Hamiltonian. It was found that the ground magnetic state is a spin liquid though the ferromagnetic state has only a slightly higher energy at melting. Analogous calculations of the magnetic phase diagram of the WC in 3D are underway [26].

V. CONCLUSION

We studied the polarization transition in the three-dimensional electron gas using twist-averaged boundary conditions and trial functions with backflow and three-body correlations. Twist-averaged boundary conditions have a much reduced systematic finite-size error, especially for the calculation of polarization energies, enabling size-converged results with fewer electrons. Using relatively small system sizes allows one to use more accurate trial wave functions and to fully converge the diffusion Monte Carlo calculations. We find a second order transition to a polarized phase at $r_s = 50 \pm 2$.

In general, methods based on the variational principle such as the fixed-node quantum Monte Carlo method for many-fermion systems, favor phases with a higher symmetry, in this case the Wigner crystal and the polarized fluid, over the more complicated unpolarized phase, (effectively a two-component mixture of spin up and down electrons.) Recall that in HF one has a polarization transition because antisymmetry is the only way to correlate electrons, however, the correlation is only between like spins; hence, there is an instability to polarize the system once the potential is dominant. But using a SJ wave function both like and unlike electrons are highly correlated. Our results demonstrate that the SJ wave functions still preferentially favor the ''simple'' phases, even using the DMC method. This symmetry argument explains the tendency of the polarized phase to become stable over a more and more restricted range of density and temperature, as more accurate methods are used. Our QMC results using the BF-3B wave function indicate that there is still an instability for spin polarization at a very low density. Although examination of the variance indicates that the polarized and unpolarized BF-3B trial functions are equally inaccurate, it is still not clear if our finding of a polarization transition is an artifact of the assumed trial wave function. Calculations with the new methods (TA and BF-3B wave functions), but with the exact fermion methods, are desirable to resolve the phase of the electron gas at intermediate densities.

ACKNOWLEDGMENTS

This research was supported by the NSF (Grant No. DMR01-04399), the Department of Physics at the University of Illinois Urbana-Champaign, and the CNRS. We acknowledge unpublished data from G. Ortiz shown in Fig. 3. Computational resources were provided by the NCSA.

[1] G. Ortiz, M. Harris, and P. Ballone, Phys. Rev. Lett. **82**, 5317 (1999).
[2] D.P. Young, Nature (London) **397**, 386 (1999).
[3] C.O. Rodriguez, R. Weht, and W.E. Pickett, Phys. Rev. Lett. **84**, 3903 (2000).
[4] S. Murakami, R. Shindou, N. Nagaosa, and A.S. Mishchenko, Phys. Rev. Lett. **88**, 126404 (2002); M.E. Zhitomirsky, T.M. Rice, and V.I. Anisimov, Nature (London) **402**, 251 (1999); L. Balents and C.M. Varma, Phys. Rev. Lett. **84**, 1264 (2000).
[5] E. Wigner, Phys. Rev. **46**, 1002 (1934).
[6] D.M. Ceperley and B.J. Alder, Phys. Rev. Lett. **45**, 566 (1980).
[7] F. Bloch, Z. Phys. **57**, 545 (1929).
[8] D. Ceperley, Phys. Rev. B **18**, 3126 (1978).
[9] B.J. Alder, D.M. Ceperley, and E.L. Pollock, Int. J. Quantum Chem. **16**, 49 (1982).
[10] The method in Ref. [1] is essentially the same as in Ref. [6], though there are several technical differences: more particles, variance minimization of short-ranged wave function rather than an analytic form with correct long-range correlations, and the use of a fixed-node method with a Slater determinant of plane waves.
[11] Y. Kwon, D.M. Ceperley, and R.M. Martin, Phys. Rev. B **58**, 6800 (1998).
[12] C. Lin, F.H. Zong, and D.M. Ceperley, Phys. Rev. E **64**, 016702 (2001).
[13] W.M.C. Foulkes, L. Mitas, R.J. Needs, and G. Rajagopal, Rev. Mod. Phys. **73**, 33 (2001).
[14] G. Ortiz, D.M. Ceperley, and R.M. Martin, Phys. Rev. Lett. **71**, 2777 (1993).
[15] T. Gaskell, Proc. Phys. Soc. London **77**, 1182 (1961).
[16] V. Natoli and D.M. Ceperley, J. Comput. Phys. **117**, 171 (1995).
[17] S. Moroni, F. H. Zong, and D. Ceperley (unpublished).
[18] Y. Kwon, D.M. Ceperley, and R.M. Martin, Phys. Rev. B **48**, 12 037 (1993).
[19] E. Stoner, Proc. R. Soc. London, Ser. A **165**, 372 (1939); **169**, 339 (1939).
[20] C. Herring, in *Magnetism*, edited by G. T. Rado and H. Suhl (Academic Press, San Diego, 1966), Vol. IV.
[21] R.A. Suris, Fiz. Tverd. Tela **3**, 1795 (1961) [Sov. Phys. Solid State **3**, 1303 (1961)].
[22] M.D. Jones and D.M. Ceperley, Phys. Rev. Lett. **76**, 4572 (1996).
[23] S. Tanaka and S. Ichimaru, Phys. Rev. B **39**, 1036 (1989); S. Ichimaru, Phys. Rev. Lett. **84**, 1842 (2000).
[24] C. Attaccalite, S. Moroni, P. Gori-Giorgi, and G. Bachelet, e-print cond-mat/0109492.
[25] B. Bernu, L. Candido, and D.M. Ceperley, Phys. Rev. Lett. **86**, 870 (2001).
[26] L. Candido, D. M. Ceperley, and B. Bernu (unpublished).